ELSEVIER

Journal of Alloys and Compounds 253–254 (1997) 101–105

Journal of ALLOYS AND COMPOUNDS

Hydrogen absorbing and desorbing properties of Nd–Fe–B and Nd–Co–B amorphous alloys

K. Tanaka*, Y. Hayashi, M. Kimura, M. Yamada

Department of Materials Science and Engineering, Nagoya Institute of Technology, Showaku, Nagoya 466, Japan

Abstract

Hydrogen absorbing and desorbing rates are measured for melt-spun Nd–Fe(or Co)–B amorphous alloys containing 5–30% Nd and 0–15% B. The hydrogen capacity changes with the Nd concentration roughly as ~3.0 H/Nd, although it is also affected by the B concentration. In alloys where Nd concentration does not exceed 20%, most of the absorbed hydrogen is desorbed from the amorphous phase. X-ray structure analysis shows that the short-range order of the amorphous alloy is maintained before and after the hydrogenation.

Keywords: Amorphous alloy; Nd–Fe(or Co)–B system; Hydrogen storage; Thermal; Desorption spectrum; Radial distribution function

1. Introduction

The ternary Nd–Fe–B and Nd–Co–B systems have attracted great interest recently because of the excellent hard-magnetic properties manifested by the isostructural $Nd_2Fe_{14}B$ and $Nd_2Co_{14}B$ compounds [1]. Hydrogen is utilized in the processing of the Nd–Fe–B hard magnets, well known as HD and HDDR processes [2] to improve the microstructures and hence their magnetic properties. The $Nd_2Fe_{14}B$ ($=Nd_{12}Fe_{82}B_6$) phase absorbs a certain amount of hydrogen which leads to a raising of the saturation magnetization and Curie temperature of the compound [3]. The Nd–Fe–B and Nd–Co–B systems have high glass-forming abilities and amorphous alloys can be readily produced by melt quenching in wide composition ranges. These amorphous alloys are expected to have higher hydrogen absorbencies than the corresponding crystalline phases, although they depend strongly on the Nd concentration. The aim of this work is to reveal their hydrogen absorbing and desorbing properties with the aim of developing a new type of hydrogen storage material. The structural and thermal properties of the hydrided amorphous alloys are also studied.

2. Experimental procedure

Amorphous alloys of $Nd_xFe_{100-x-y}B_y$ ($x=15$, 20 $y=0$, 5, 10, 15) and $Nd_xCo_{85-x}B_{15}$ ($x=5$, 10, 15, 20, 25, 30) were produced by melt spinning in the form of ribbons (~1 mm wide and ~20 μm thick). In these systems, the addition of boron is important, especially for the Nd–Co system with low Nd concentration ($x \leqq 25$), in enhancing the glass formability and thermal stability, although it partly reduces the hydrogen absorbency. The glass formation was checked by X-ray diffraction. The samples were exposed to H_2 gas of 1 MPa at 393–423 K without any pretreatment, and hydrogen absorbing rates were measured with a volumetric method. All the samples remained amorphous after the hydriding. The desorbing process was observed using thermal desorption spectrometry (TDS). In this technique, a piece of hydrided ribbon is heated at a constant rate (0.17 $K\,s^{-1}$) in a dynamic high-vacuum system, and the hydrogen partial pressure in the chamber which corresponds to the hydrogen desorption rate is recorded as a function of temperature. The crystallization temperature, T_x, was determined by DSC measurements. X-ray structure analyses were carried out for some of these hydrogenated amorphous alloys.

3. Results and discussion

Figs. 1 and 2 show the amounts of hydrogen absorption as a function of holding time for the Nd–Fe–B and Nd–Co–B amorphous alloys, respectively. In the Nd–Fe–

*Corresponding author.

PII S0925-8388(96)03060-5

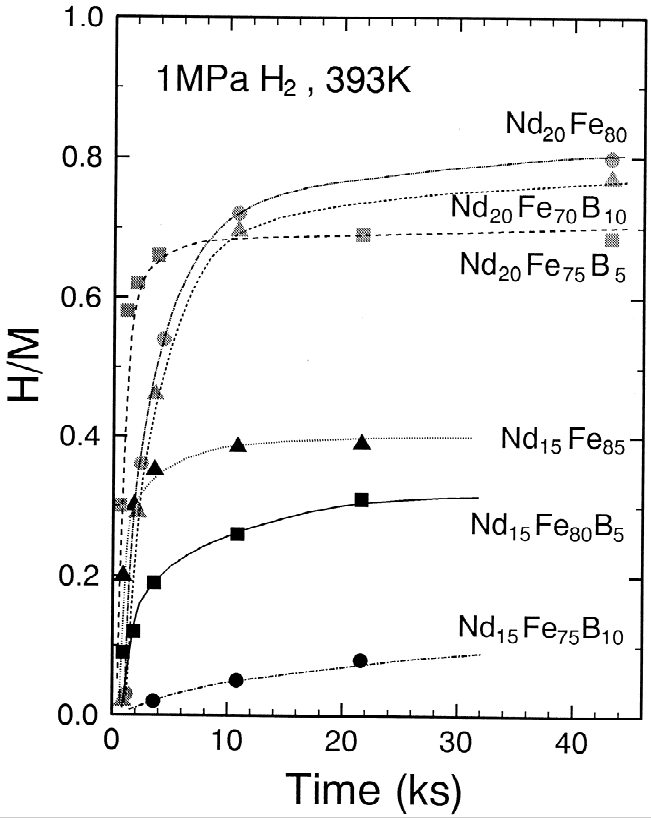

Fig. 1. Hydrogen absorption in Nd–Fe and Nd–Fe–B amorphous alloys under 1 MPa H_2 at 393 K as a function of holding time.

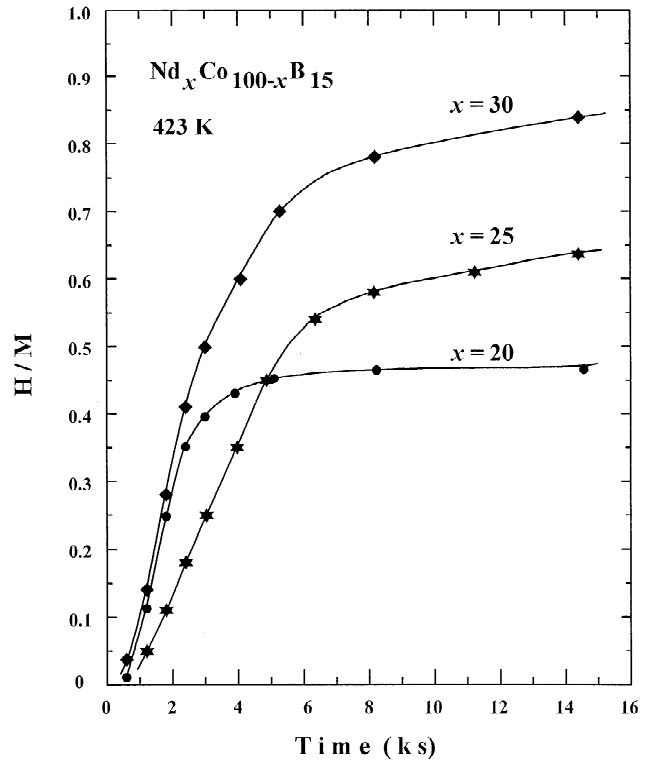

Fig. 2. Hydrogen absorption in Nd–Co–B amorphous alloys under 1 MPa H_2 at 423 K as a function of holding time.

B alloys, the hydrogen capacity reaches H/M~0.4 for $Nd_{15}Fe_{85}$ and ~0.8 for $Nd_{20}Fe_{80}$, both of which tend to decrease with B addition. Thus the average capacity per Nd atom, H/Nd, is roughly 2.5–3.5. In the Nd–Co–B amorphous alloys, on the other hand, the hydrogen capacity increases from ~0.45 for $Nd_{20}Co_{65}B_{15}$ to ~0.85 for $Nd_{30}Co_{55}B_{15}$, for which H/Nd ranges from 2.3–2.8. The absorbing rates are similar in both alloy systems.

Fig. 3 shows TDS spectra for the Nd–Fe–B amorphous alloys hydrided to near the maximum capacities. The crystallization temperatures are indicated with arrows in the figures. It increases with increasing B concentration from ~700 K to ~900 K. The main crystallization products, as examined by X-ray diffraction, were Nd_2Fe_{17} in the binary alloys and $Nd_2Fe_{14}B$ in the ternary alloys. Some unidentified phases are also involved in both products. In each alloy, the main TDS peak appears between 400 and 600 K, well below the crystallization temperature. This peak represents hydrogen desorption from the amorphous phase and we find that ~80% of the stored hydrogen is desorbed from the amorphous phase in these alloys. Another peak, much smaller than the main peak, appears well above T_x, which is probably caused by the decomposition of NdH_x formed via a disproportionation reaction of

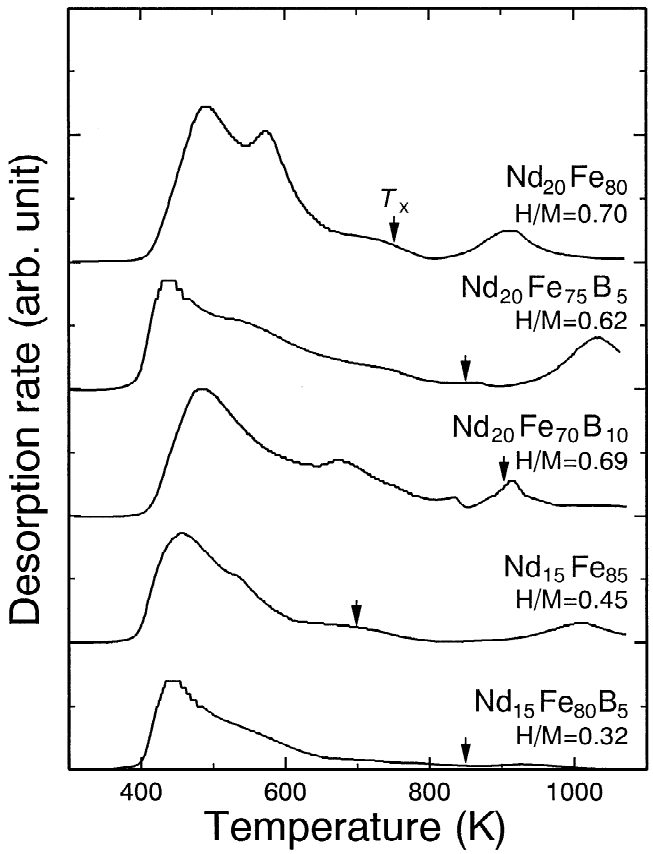

Fig. 3. Thermal desorption spectra of Nd–Fe and Nd–Fe–B amorphous alloys hydrided to near the maximum capacities. The crystallization temperatures T_x are indicated by the arrows.

the crystallization products with the remaining hydrogen at temperatures above T_x.

Fig. 4 shows similar spectra for the Nd–Co–B amorphous alloys. In these alloys, T_x falls at ~580 K, appreciably lower than those of the Nd–Fe–B alloys, irrespective of the Nd concentration. The desorption from the amorphous phase occurs between 350 and 550 K, followed by a second peak (600–700 K) which increases with increasing Nd concentration. The origin of the latter peak is not clear at present, but it may be attributed to hydrogen desorption from certain crystallization products such as $NdCo_3$ and some ternary borides. Above 700 K, other small peaks are also seen, and they might be due to the decomposition of more stable hydrides such as NdH_x. These spectra show that, although the stored hydrogen increases with Nd concentration, the amount of desorption from the amorphous phase (peak area) remains almost constant ($\Delta H/M = 0.25–0.30$). Fig. 5 shows the TDS spectra for amorphous $Nd_{20}Co_{65}B_{15}$ charged with different amounts of hydrogen. It can clearly be seen that the desorption peak from the amorphous phase increases with increasing stored hydrogen and shifts toward lower temperatures, a general feature of TDS peaks of amorphous alloys. It manifests some fine structure possibly reflecting a distribution of hydrogen site energies in the amorphous alloy.

Fig. 6 shows radial distribution functions, RDF(r), for the $Nd_{20}Co_{65}B_{15}$ amorphous alloys measured before and after hydriding to the same amounts as those shown in Fig. 5. This function describes a weight-averaged number of atoms within a spherical shell of unit thickness with a radius r about a central atom. Due to great differences in

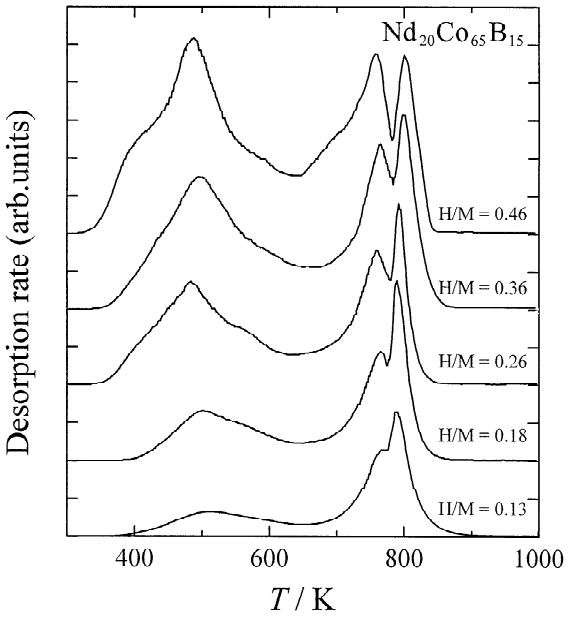

Fig. 5. Thermal desorption spectra of $Nd_{20}Co_{65}B_{15}$ amorphous alloys loaded with different amounts of hydrogen.

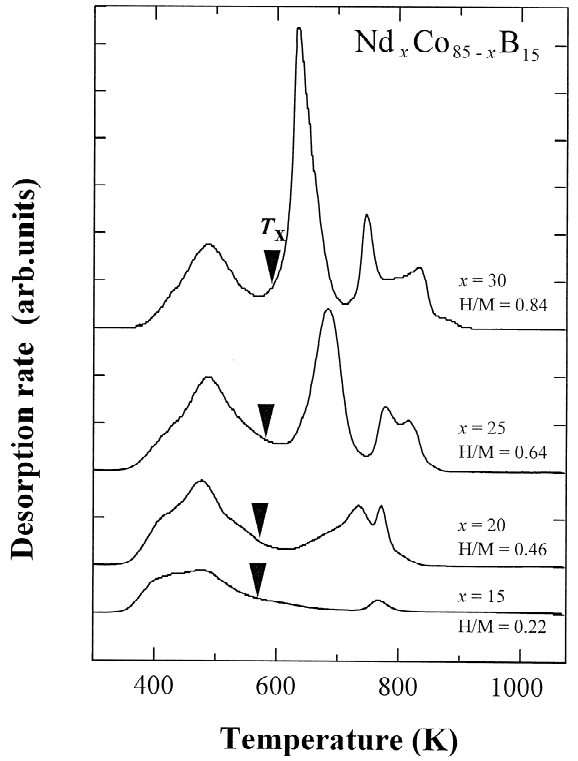

Fig. 4. Thermal desorption spectra of Nd–Co–B amorphous alloys hydrided to near the maximum capacities. The crystallization temperatures T_x are indicated by the arrows.

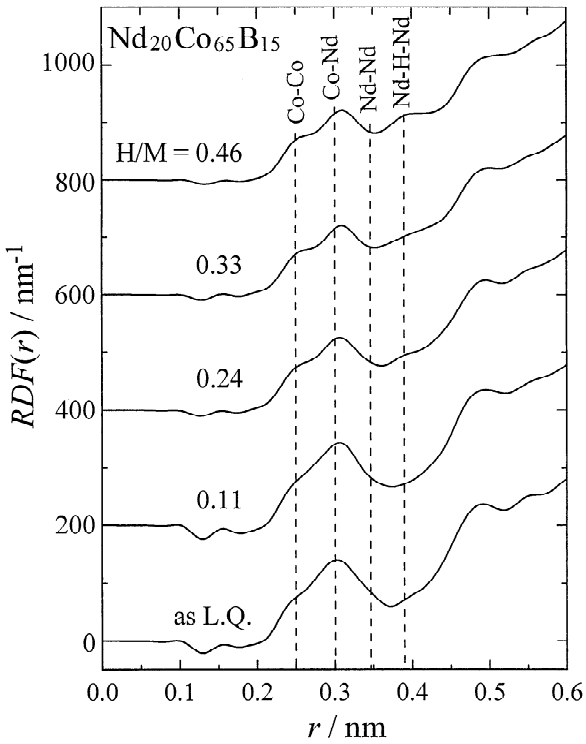

Fig. 6. Radial distribution functions, RDF(r), for $Nd_{20}Co_{65}B_{15}$ amorphous alloys before and after hydriding to the same levels as those shown in Fig. 5.

the atomic scattering factors and concentrations of the constituting elements, only the Co–Co, Co–Nd and Nd–Nd pair correlations (out of six partial pair correlations in total) are dominantly involved to give the RDF(r) for this alloy. The contact distances of the pairs estimated from their atomic radii are $d_{Co-Co}=0.25$ nm, $d_{Co-Nd}=0.31$ nm and $d_{Nd-Nd}=0.36$ nm, from which the first and second peaks of the as prepared amorphous alloy are identified as the Co–Co and Co–Nd pairs in the first coordination shell, respectively. Although a peak corresponding to the Nd–Nd pair is not clearly seen owing to its relatively small weighting factor, the peak becomes manifest in the RDF(r) for the $Nd_{25}Co_{60}B_{15}$ and $Nd_{30}Co_{55}B_{15}$ amorphous alloys (not shown in the figure). As the amorphous alloy is hydrided, certain profile changes are induced; while the Co–Co and Co–Nd peaks changes little with increasing hydrogen content, the Nd–Nd component is reduced in amplitude and a new peak (labeled as Nd–H–Nd) develops at $r=\sim0.39$ nm instead. The Co–Nd peak is also slightly shifted toward a higher r value. According to a more elaborate analysis based on the least-squares fitting with a combination of Gaussian peaks [4], the coordination number for each pair is calculated as: $Z_{Co-Co}=6.9$, $Z_{Co-Nd}=3.1$ and $Z_{Nd-Nd}=4.5$ before hydriding and $Z_{Co-Co}=7.0$, $Z_{Co-Nd}=2.9$, $Z_{Nd-Nd}=1.0$ and $Z_{Nd-H-Nd}=3.5$ after hydriding to H/M=0.46. From this analysis, we find that $Z_{Nd-Nd}+Z_{Nd-H-Nd}$, as well as Z_{Co-Co} and Z_{Co-Nd}, is kept almost constant irrespective of the hydrogen content. This means that the short-range order (SRO) of the Nd–Co–B amorphous alloy is not altered significantly by the hydriding, if we interpret the Nd–H–Nd peak to arise from a Nd–Nd pair involving a hydrogen atom in between. A similar analysis has been performed for hydrided Nd–Fe–B amorphous alloys [5], and a consistent result has been obtained.

It has been shown in our previous study [6] that Nd–Fe–B amorphous alloys have a structural unit of trigonal prism which is also present in $Nd_2Fe_{14}B$ crystal. From the similarity of RDF(r) between the Nd–Fe–B and Nd–Co–B amorphous alloys, the latter is also expected to have a similar structural unit to the former. Fig. 7 shows a sketch of local structure about the trigonal prism in the Nd_2Fe(or $Co)_{14}B$ crystal [1]. A boron atom is surrounded by six Fe(Co) atoms forming a trigonal prism with three further Nd atoms capping the prism. According to a neutron diffraction study of a hydrided $Nd_2Fe_{14}B$ compound [7], H atoms enter the Nd_3Fe_1 and Nd_2Fe_2 type tetrahedral sites outside the prism forming the $Nd_2Fe_{14}BH_5$ hydride. Taking into account the similarity of the SRO between the compound and the amorphous alloy, hydrogen atoms absorbed in a Nd–Fe–B or Nd–Co–B amorphous alloy are expected to occupy $Nd_3Fe(Co)_1$ and $Nd_2Fe(Co)_2$ sites, together with $Nd_1Fe(Co)_3$ and Nd_4 tetrahedral sites which should also be present in the amorphous alloy. Hydrogen atoms occupying these sites interact chiefly with Nd atoms and locally expand the Nd–Nd bonds significantly and the Co–Nd bonds slightly. This explains well, why the original Nd–Nd peak of RDF(r) is reduced but instead a new peak (Nd–H–Nd) is developed at a longer radial distance without changing the net coordination number. The hydrogen atoms trapped at the Nd_4 sites may be too stable to be desorbed before the crystallization. They should remain in certain crystallization products and be desorbed at temperatures higher than the T_x.

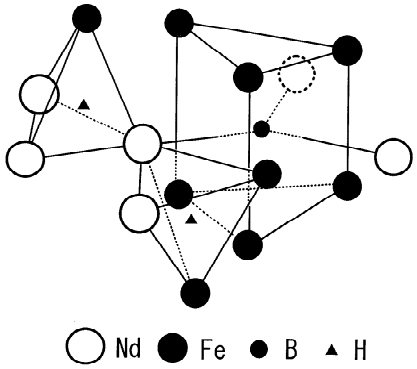

Fig. 7. A local structure existing in Nd_2Fe (or $Co)_{14}B$ compound, showing a trigonal prism and two kinds of tetrahedral sites where hydrogen atoms are accommodated.

4. Conclusion

Ternary Nd–Fe–B and Nd–Co–B amorphous alloys produced by melt spinning readily absorb hydrogen under 1 MPa H_2 at 393–423 K. The hydrogen capacity increases with Nd concentration roughly at ~3.0 H/Nd. Addition of 5–15% B is important in stabilizing the amorphous structure, although it tends to reduce the hydrogen capacity by certain amounts. If the Nd concentration does not exceed 20%, most of the absorbed hydrogen is desorbed before the crystallization takes place ($T_x>\sim600$ K), the desorbing rate attaining a maximum at 450–500 K. Hydrogen atoms enter tetrahedral interstices such as $Nd_2Fe(Co)_2$, $Nd_3Fe(Co)_1$ and Nd_4 in the amorphous alloy and combine with Nd atoms extending the Nd–Nd bond lengths. The short-range order of the amorphous alloy is not altered significantly by the hydriding. Further study is necessary to improve the hydrogen absorbing and desorbing characteristics of these amorphous alloys.

Acknowledgments

This work has partly been supported by the Grant-in-Aid for Scientific Research from the Ministry of Education, Science and Culture of Japan.

References

[1] J.F. Herbst, *Rev. Mod. Phys., 63* (1991) 819.
[2] I.R. Harris and P.J. McGuiness, *J. Less-Common Met., 172–174* (1991) 1273.
[3] L. Pareti, O. Moze, D. Fruchart, Ph. L'Heritier and A. Yaouanc, *J. Less-Common Met., 142* (1988) 187.
[4] Y. Hayashi, M. Yamada and K. Tanaka, in preparation.
[5] Y. Narita, M. Yamada and K. Tanaka, *Mater. Trans. JIM, 36* (1995) 1193.
[6] M. Yamada, Y. Terashima and K. Tanaka, *Mater. Trans. JIM, 34* (1993) 895.
[7] O. Isnard, W.B. Yelon, S. Miraglia and D. Fruchart, *J. Appl. Phys., 78* (1995) 1892.